Repulsion Exerted on a Spherical Particle by a Polymer Brush

Jaeup U. Kim* and Mark W. Matsen*,†

Department of Mathematics, University of Reading, Whiteknights, Reading RG6 6AX, U.K.

Received August 22, 2007; Revised Manuscript Received October 25, 2007

ABSTRACT: The steric repulsion exerted on spherical particles by a semidilute polymer brush is evaluated using numerical self-consistent field theory (SCFT) in cylindrical coordinates. This accurate treatment provides the opportunity to test the conventional analytical approach, where the strong-stretching theory (SST) of Milner, Witten, and Cates for uniform compression can be adapted to particles of any shape using the Derjaguin approximation. While the Derjaguin approximation works well, at least, for the interaction energy, the SST proves to be seriously inaccurate for realistic grafting densities. Nevertheless, an efficient and accurate treatment for arbitrarily shaped particles remains possible if the uniform compression in the Derjaguin approximation is supplied by SCFT.

I. Introduction

Polymer brushes, formed by densely grafting polymers to a surface, produce a steric repulsion when deformed, which offers a convenient means of countering van der Waals attractions.[1] Brushes now provide a routine method of stabilizing colloidal suspensions,[2] and are being investigated as a way of preventing adsorption on surfaces by nanoparticles and macromolecules such as proteins.[3,4] Experiments have examined the steric repulsion by specially designed surface force apparatus (SFA) that measure the interaction between two weakly curved surfaces[4−8] and by the highly curved tips of standard atomic force microscopes (AFM),[9] and there seems to be reasonable agreement with theory.

The theoretical predictions are generally provided by calculating the repulsion of uniform compression, and then adapting it to the nonuniform geometry by applying the standard Derjaguin approximation.[10] The uniform compression is typically treated by either the simple scaling theory of Alexander and de Gennes[11] or by the strong-stretching theory (SST) of Milner, Witten, and Cates.[12] The earlier scaling theory is regarded as the less rigorous treatment, because it assumes a steplike profile with all the chain ends located at the outer extremity of the brush, whereas the SST allows the profile and end-segment distribution to adjust in response to the compression. Furthermore, the SST makes definitive predictions, while the scaling theory only predicts the functional form of the interaction. As it turns out, the scaling theory often performs as well as or better than the SST,[4−6,13,14] but this can be attributed to the use of fitting parameters.

There are two separate sources of inaccuracy to consider in this type of calculation. The first is that associated with the Derjaguin approximation, which assumes surfaces of low curvature. It remains unclear how large the curvature can become before the approximation fails; it is certainly fine for SFA measurements but is questionable when applied to AFM tips.[15,16] The second issue is the use of SST for the uniform compression, which makes an unrealistic assumption that the polymer chains are restricted to so-called *classical* trajectories. Typical experiments[5−8] come nowhere near the grafting densities required for this assumption,[17] and there is theoretical evidence[18] that this results in considerable inaccuracy.

* Corresponding author. E-mail: j.kim@reading.ac.uk.
† E-mail: m.w.matsen@reading.ac.uk.

Here the steric force exerted on spherical particles by a semidilute polymer brush is calculated using the numerical self-consistent field theory (SCFT)[19] in cylindrical coordinates (see Figure 1). This approach explicitly treats the particle shape and sums over all possible polymer trajectories, providing more accurate predictions for small particles and realistic grafting densities. The principle aim of this initial paper is to investigate the inaccuracies associated with the Derjaguin and strong-stretching approximations.

II. Theory

This section presents our underlying theoretical model for a spherical particle of radius R impinging upon a flat polymer brush in a solvent background as depicted in Figure 1. The brush is assumed to have a fixed uniform grafting density of $\sigma \equiv n/\mathcal{A}$, where n is the total number of polymer chains and $\mathcal{A}$ is the surface area of the substrate. The polymers are treated as flexible Gaussian chains[19] each with a natural end-to-end length of $aN^{1/2}$, where a is the statistical segment length and N is the number of segments per chain. For simplicity, we assume that the particle and the substrate have no significant surface affinity for either the polymer or the solvent, and thus they are regarded as inert impenetrable objects. If necessary, a surface potential can easily be incorporated into the theory.

To perform statistical mechanics on this system,[17] the configuration of the α'th chain is denoted by the space curve, $\mathbf{r}_\alpha(s)$, where s is a parameter that runs along the backbone of

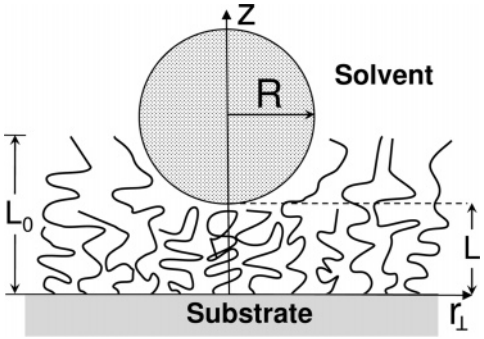

Figure 1. Schematic diagram of a polymer brush of thickness L_0 compressed by a spherical particle of radius R at a distance L above the substrate. Positions are specified in cylindrical coordinates, ($r_\perp$, θ, z), to take advantage of the axial symmetry in θ.

10.1021/ma071906t CCC: $40.75
Published on Web 12/05/2007

the polymer from 0 at the free end to 1 at the grafted end. This allows the total polymer concentration to be specified as

$$\hat{\phi}(\mathbf{r}) = \frac{N}{\rho_0}\sum_{\alpha=1}^{n}\int_0^1 \mathrm{d}s\ \delta(\mathbf{r}-\mathbf{r}_\alpha(s)) \tag{1}$$

where ρ_0^{-1} is the volume occupied by each segment. The thermodynamic average of the brush profile, $\langle\hat{\phi}(\mathbf{r})\rangle$ is calculated in the mean-field approximation, where the molecular interactions experienced by the segments are approximated by a static field

$$w(\mathbf{r}) = \upsilon N\langle\hat{\phi}(\mathbf{r})\rangle \tag{2}$$

Note that the excluded-volume parameter, υ, is assumed to be sufficiently positive (i.e., good solvent) so as to swell the brush to semidilute conditions.[12,17]

For convenience, the grafting density, σ, can be removed from the problem by defining the scaled concentration

$$\phi(\mathbf{r}) = \frac{a\rho_0}{\sigma N^{1/2}}\langle\hat{\phi}(\mathbf{r})\rangle \tag{3}$$

normalized such that

$$\int \mathrm{d}\mathbf{r}\ \phi(\mathbf{r}) = \mathscr{A}aN^{1/2} \tag{4}$$

This allows the field eq 2 to be rewritten as

$$w(\mathbf{r}) = \Lambda\phi(\mathbf{r}) \tag{5}$$

in terms of the reduced interaction parameter

$$\Lambda \equiv \frac{\upsilon\sigma N^{3/2}}{a\rho_0} \tag{6}$$

Likewise, the molecular-weight dependence, N, can be scaled out of the problem by dividing all lengths (e.g., R, L, $r_\perp$, and z) by $aN^{1/2}$. In the end, our model is described by just three parameters: Λ, $R/aN^{1/2}$, and $L/aN^{1/2}$. Later in this section, we will substitute the parameter Λ by $L_0/aN^{1/2}$, where L_0 is the classical brush height defined by SST.

A. Self-Consistent Field Theory (SCFT). The full mean-field theory for flexible Gaussian chains is generally referred to as self-consistent field theory (SCFT),[20] and numerical solutions for polymer brushes have been available for more than a decade.[17,18,21,22] These earlier calculations considered uniform brushes, where the grafted ends are allowed to float freely in a two-dimensional plane a small distance ϵ above the substrate (see ref 17 for an explanation of why ϵ must be nonzero). Here the lateral symmetry is broken by the spherical particle, and therefore we must instead follow a derivation that strictly enforces the uniform grafting density.[23]

The starting point of a SCFT calculation is the partition function for a chain fragment of sN segments with its ends fixed at $\mathbf{r}$ and $\mathbf{r}'$. It is defined by

$$q(\mathbf{r},\mathbf{r}',s) \propto \int \mathscr{D}\mathbf{r}_\alpha \exp\left(-\frac{E[\mathbf{r}_\alpha;s]}{k_\mathrm{B}T}\right)\times \delta(\mathbf{r}_\alpha(0)-\mathbf{r}')\delta(\mathbf{r}_\alpha(s)-\mathbf{r}) \tag{7}$$

where the energy of a given configuration is

$$\frac{E[\mathbf{r}_\alpha;s]}{k_\mathrm{B}T} = \int_0^s \mathrm{d}t\left(\frac{3}{2a^2N}\left|\frac{\mathrm{d}}{\mathrm{d}t}\mathbf{r}_\alpha(t)\right|^2 + w(\mathbf{r}_\alpha(t))\right) \tag{8}$$

Rather than using the path integral in eq 7, the partition function is more efficiently evaluated by solving a modified diffusion equation,[19,20]

$$\frac{\partial}{\partial s}q(\mathbf{r},\mathbf{r}',s) = \left[\frac{a^2N}{6}\nabla^2 - w(\mathbf{r})\right]q(\mathbf{r},\mathbf{r}',s) \tag{9}$$

subject to the initial condition

$$q(\mathbf{r},\mathbf{r}',0) = \delta(\mathbf{r}-\mathbf{r}')a^3N^{3/2} \tag{10}$$

The impenetrability of the particle and the substrate is accounted for by enforcing the Dirichlet boundary condition, $q(\mathbf{r},\mathbf{r}',s) = 0$, at $r_\perp^2 + (z-L-R)^2 = R^2$ and $z = 0$.

In terms of the partition function, the average segment concentration from a single chain grafted at $\mathbf{r}'$ is given by

$$\phi(\mathbf{r};\mathbf{r}') = \frac{\int_0^1 \mathrm{d}s\ q_\mathrm{f}(\mathbf{r},s)q(\mathbf{r},\mathbf{r}',1-s)}{q_\mathrm{f}(\mathbf{r}',1)} \tag{11}$$

where

$$q_\mathrm{f}(\mathbf{r},s) \equiv \frac{1}{a^3N^{3/2}}\int \mathrm{d}\mathbf{r}'\ q(\mathbf{r},\mathbf{r}',s) \tag{12}$$

is the partition function for a chain fragment with one free end. Since it is just a linear combination of $q(\mathbf{r},\mathbf{r}',s)$, it satisfies the diffusion eq 9 with the Dirichlet boundary condition, but eqs 10 and 12 imply a different initial condition of $q_\mathrm{f}(\mathbf{r},0) = 1$. Note that the free-end distribution of the chain is

$$g(\mathbf{r};\mathbf{r}') = \frac{q(\mathbf{r},\mathbf{r}',1)}{q_\mathrm{f}(\mathbf{r}',1)} \tag{13}$$

The average polymer concentration for the entire brush is then given by the integral

$$\phi(\mathbf{r}) = \frac{1}{a^2N}\int \mathrm{d}\mathbf{r}'\ \delta(z'-\epsilon)\phi(\mathbf{r};\mathbf{r}') \tag{14}$$

$$= \int_0^1 \mathrm{d}s\ q_\mathrm{f}(\mathbf{r},s)q_\mathrm{g}(\mathbf{r},1-s) \tag{15}$$

where we have made the convenient definition

$$q_\mathrm{g}(\mathbf{r},s) \equiv \frac{1}{a^2N}\int \mathrm{d}\mathbf{r}'\ \delta(z'-\epsilon)\frac{q(\mathbf{r},\mathbf{r}',s)}{q_\mathrm{f}(\mathbf{r}',1)} \tag{16}$$

representing the partition function for a grafted portion of the chain. Similarly, $q_\mathrm{g}(\mathbf{r},s)$ obeys the diffusion eq 9 with the Dirichlet boundary condition, and it must satisfy the initial condition

$$q_\mathrm{g}(\mathbf{r},0) = \frac{\delta(z-\epsilon)aN^{1/2}}{q_\mathrm{f}(\mathbf{r},1)} \tag{17}$$

according to eqs 10 and 16. This function also has the useful property that it provides the distribution

$$g(\mathbf{r}) = q_\mathrm{g}(\mathbf{r},1) \tag{18}$$

of all the polymer free ends.

Once the field, $w(\mathbf{r})$, has been adjusted such that $\phi(\mathbf{r})$ satisfies eq 5, the free energy of the system is given by

$$\frac{F(L;R)}{k_BT} = -\sigma \int d\mathbf{r}\, \delta(z-\epsilon) \ln q_f(\mathbf{r}, 1) - \frac{\sigma}{2aN^{1/2}} \int d\mathbf{r}\, w(\mathbf{r})\phi(\mathbf{r}) \quad (19)$$

The first term integrates the single-chain free energy, $-k_BT \ln q_f(\mathbf{r}, 1)$, over the grafting distribution, $\sigma\delta(z-\epsilon)$, while the second term subtracts half of the field energy to correct for the usual double counting of the internal energy that occurs in mean-field theory.

To solve the diffusion eq 9, we implement a Crank-Nicholson algorithm in cylindrical coordinates, $(r_\perp, \theta, z)$. Because of the axial symmetry involved, none of our quantities have any θ dependence and therefore the SCFT reduces to a 2-dimensional computation. In the limit of uniform compression (i.e., $R \to \infty$), the $r_\perp$ dependence also disappears reducing the SCFT to a quick 1-dimensional computation. In order to obtain accurate results, we employ a fine mesh (typically $\Delta r_\perp = 0.03aN^{1/2}$, $\Delta z = 0.01aN^{1/2}$, and $\Delta s = 0.00125$) and use a generous system size (up to $r_\perp = 15aN^{1/2}$ and $z = 6aN^{1/2}$). For efficiency, the Crank-Nicholson method is done by the usual operator-splitting technique,[24] where a half time-step is done treating $r_\perp$ implicitly and z explicitly and then vice versa for the next half time-step. We find that the conservation of polymer is best maintained by not splitting the field term and only having it appear at the integer time-steps. To further improve the conservation of material, all volume integrals, $\int d\mathbf{r}\, f(\mathbf{r})$, are performed by a simple quadrature where the integrand, $f(r_\perp, z)$, at each grid point is weighted by the volume of its own cell (defined as the region of space closest to that particular grid point). The Anderson-mixing algorithm[25] provides an efficient method of satisfying the self-consistent field condition, eq 5.

B. Strong-Stretching Theory (SST). For strongly stretched brushes, the chains are eventually limited to the configurations that minimize $E[\mathbf{r}_\alpha; 1]$. For an unperturbed brush, these ground-state trajectories are straight paths, $z_\alpha(s)$, in the vertical direction. Using an analogy with classical mechanics, Milner, Witten, and Cates[12] argued that in this limit the mean field must adopt the harmonic potential

$$w(z) = \frac{3\pi^2(C-z^2)}{8a^2N} \quad (20)$$

for which the *classical* trajectories are

$$z_\alpha(s) = z_0 \cos(\pi s/2) \quad (21)$$

where z_0 denotes the position of the free end. (Note that Semenov[26] derived this potential several years earlier for melt brushes using a variational approach, which is easily generalized to include solvent.[27]) In the absence of compression, $z = \sqrt{C} \equiv L_0$ defines the point at which the polymer concentration vanishes. This combined with eq 4 predicts a *classical* brush height relative to the characteristic polymer size of

$$\frac{L_0}{aN^{1/2}} = \left(\frac{4\Lambda}{\pi^2}\right)^{1/3} \quad (22)$$

From now on, we will characterize our brushes by this ratio rather than the less intuitive Λ parameter.

For uniform compressions of $L < L_0$, the potential remains harmonic but the constant adjusts according to

$$C = \frac{2L_0^3}{3L} + \frac{1}{3}L^2 \quad (23)$$

so as to satisfy eq 4. The free energy of the compressed brush is then obtained by taking the energy of a single chain in the field, $E[\mathbf{r}_\alpha, 1] = 3\pi^2C/8a^2N$ for all values of z_0, and subtracting half the field energy (i.e., the second term in eq 19). This leads to the simple analytical formula[1,12]

$$\frac{F(L;\infty)}{nk_BT} = \frac{9\pi^2L_0^2}{40a^2N} h(L/L_0) \quad (24)$$

where

$$h(u) \equiv (5u^{-1} + 5u^2 - u^5)/9 \quad (25)$$

for $u \le 1$ and is one otherwise.

Unfortunately, the exact SST solution for a brush in contact with a spherical particle is intractable. The classical trajectories become curved with the loss of lateral symmetry, and consequently the argument for the parabolic potential breaks down. Although there have been a number of SST calculations[15,28−30] dealing with nonuniform brushes, they all involve additional approximations and assumptions.

C. Derjaguin Approximation. The well-known Derjaguin approximation[10] provides a convenient means of estimating the properties of nonuniform compression in terms of uniform compression. This is accomplished by assuming that the local details beneath the particle at $r_\perp$ are well approximated by a brush uniformly compressed to

$$l(r_\perp) = L + R - \sqrt{R^2 - r_\perp^2} \quad (26)$$

the vertical separation between the substrate and the particle. The method can be used in either the SCFT or SST framework, provided the particle is large enough that $l(r_\perp)$ is a slowly varying function over the contact area, $r_\perp \lesssim \sqrt{R^2-(R+L-L_0)^2}$. If this condition is satisfied, then the interaction energy can be estimated as

$$\Delta F(L;R) = \sigma \int_0^R dr_\perp\, 2\pi r_\perp\, \Delta f(l(r_\perp)) \quad (27)$$

where

$$\Delta f(l) \equiv [F(l;\infty) - F(\infty;\infty)]/n \quad (28)$$

is the free energy penalty per chain for a brush uniformly compressed to a height of l.

The form of the Derjaguin approximation in eq 27 is easily generalized to particles of any shape, but a further simplification is possible for the special case of spherical particles. Continuing to assume large radii, we invoke the Taylor series approximation, $\sqrt{R^2-r_\perp^2} \approx R(1 - r_\perp^2/2R^2)$, and switch the integration variable from $r_\perp$ to l; this transforms eq 26 into the simpler expression

$$\Delta F(L;R) = 2\pi\sigma R \int_L^\infty dl\, \Delta f(l) \quad (29)$$

which depends linearly on the particle size, R. For SST, the integral can be performed analytically, giving

$$\frac{\Delta F(L;R)}{k_BT} = \frac{9\pi^3\sigma R L_0^3}{20a^2N} H(L/L_0) \quad (30)$$

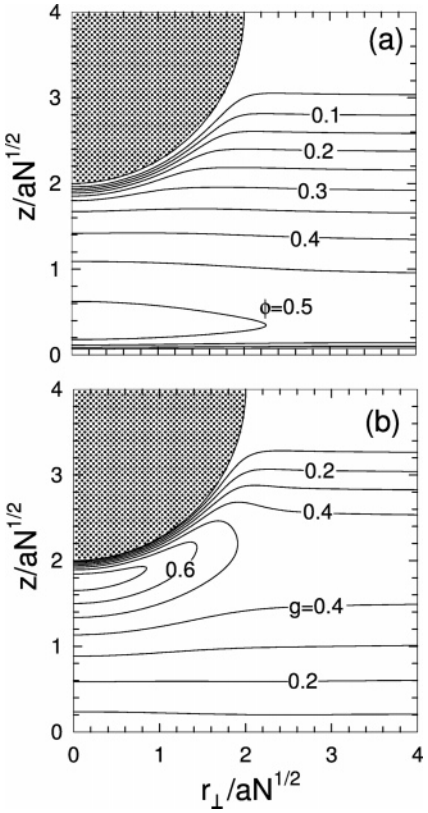

Figure 2. Contour plots of (a) the polymer concentration, $\phi(r_\perp, z)$, and (b) the end-segment distribution, $g(r_\perp, z)$, calculated with the full SCFT for a brush of thickness, $L_0 = 3aN^{1/2}$, compressed by a particle of radius, $R = 2aN^{1/2}$, at a distance, $L = 2aN^{1/2}$, above the grafting surface. Note that some ϕ contours next to the substrate have been omitted for clarity.

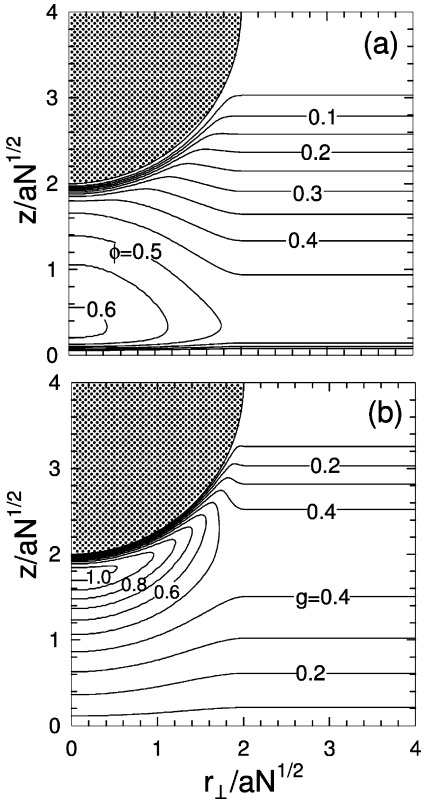

Figure 3. Analogous plots to those in Figure 2, but obtained in the Derjaguin approximation where $\phi(r_\perp, z)$ and $g(r_\perp, z)$ are estimated at each value of $r_\perp$ by a 1-dimensional SCFT calculation for a uniform compression of $l(r_\perp)$.

where

$$H(u) \equiv (-45 - 30 \ln u + 54u - 10u^3 + u^6)/54 \quad (31)$$

for $u \leq 1$ and is zero otherwise. A nice feature of eq 29 is that it provides a simple expression for the force on a large spherical particle

$$\text{force} \equiv -\frac{\mathrm{d}}{\mathrm{d}L}\Delta F(L; R) = 2\pi\sigma R \Delta f(L) \quad (32)$$

that only involves calculating the uniform compression for a single brush height of L. One will often see eq 32 referred to as the Derjaguin approximation, even though it is in reality a restricted version.

III. Results

We begin our study by examining a particle of radius $R = 2aN^{1/2}$ positioned a distance $L = 2aN^{1/2}$ above a substrate grafted with a brush of thickness $L_0 = 3aN^{1/2}$. (Note that this refers to the classical brush thickness predicted by SST; the actual profile includes a tail that extends a characteristic distance, $\xi = L_0^{-1/3}a^{4/3}N^{2/3}$, beyond L_0.[17,31]) Figure 2 shows the brush profile, $\phi(r_\perp, z)$, and corresponding end-segment distribution, $g(r_\perp, z)$, obtained from a full 2-dimensional SCFT calculation. Although the impenetrability causes the polymer concentration to vanish at the substrate and the particle surface, it does recover quickly. The depletion zone next to the substrate has a small width of $\mu = a^2N/4L_0$,[17] and the concentration next to the particle recovers to ϕ_∞ in a short distance that scales as $\xi_{MF} \sim (\upsilon a \phi_\infty)^{-1/2}$.[32]

It is remarkable how there is almost no buildup of material directly beneath the particle, as evident from the negligible effect the particle has on the equi-concentration contour, $\phi(r_\perp, z) = 0.4$. There is a more significant accumulation of end-segments directly below the particle, but the $g(r_\perp, z) = 0.4$ contour is still reasonably flat. Clearly a considerable amount of polymer has been displaced from under the particle, but this happened without any significant disturbance beyond the contact zone (i.e., $r_\perp \gtrsim 1.7aN^{1/2}$). The reason is that the displaced segments are spread over a relatively large area, on account of the fact that the amount of brush between $r_\perp$ and $r_\perp + dr_\perp$ increases linearly with $r_\perp$. This response by the polymer concentration is in stark contrast to the predictions in Figure 3 based on the Derjaguin assumption, where $\phi(r_\perp, z)$ and $g(r_\perp, z)$ at $r_\perp$ are approximated by a uniformly compressed brush of thickness $l(r_\perp)$. The difference is attributed to the fact that the Derjaguin approximation prevents the lateral displacement of segments.

The validity of the Derjaguin assumption is most easily assessed by Figure 4, where the concentration profiles, $\phi(0,z)$, directly below particles of different radii, R, are compared with that of uniform compression (dashed curve). Unfortunately the convergence is very slow; even at $R = 30aN^{1/2}$, there is still a significant gap between the 1- and 2-dimensional SCFT profiles. This can be understood by examining Figure 5, which shows the contributions from a single polymer chain, eqs 11 and 13, grafted directly beneath a particle of radius $R = 2aN^{1/2}$. It is affected by the curvature of the particle due to the fact its concentration extends laterally to about $r_\perp \approx aN^{1/2}$, but this is not the main source of the slow convergence. The problem is that $\phi(0, z)$ and $g(0, z)$ receive a significant contribution from chains grafted as far away as $r_\perp \approx aN^{1/2}$, where the vertical separation has increased by about 10%. This inaccuracy in the Derjaguin approximation will persist until R is sufficiently large

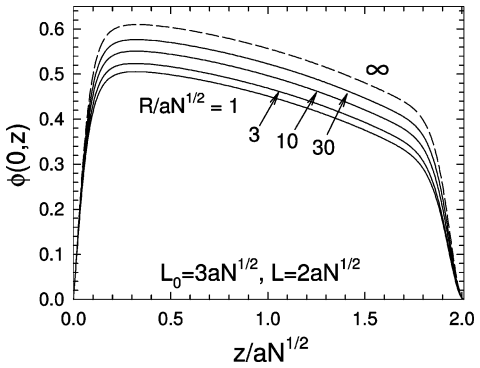

Figure 4. Polymer concentration, $\phi(0, z)$, directly beneath (i.e., $r_\perp = 0$) particles of various radii, R, each compressing the brush from a thickness of $L_0 = 3aN^{1/2}$ down to $L = 2aN^{1/3}$. The dashed curve denotes the limit of uniform compression.

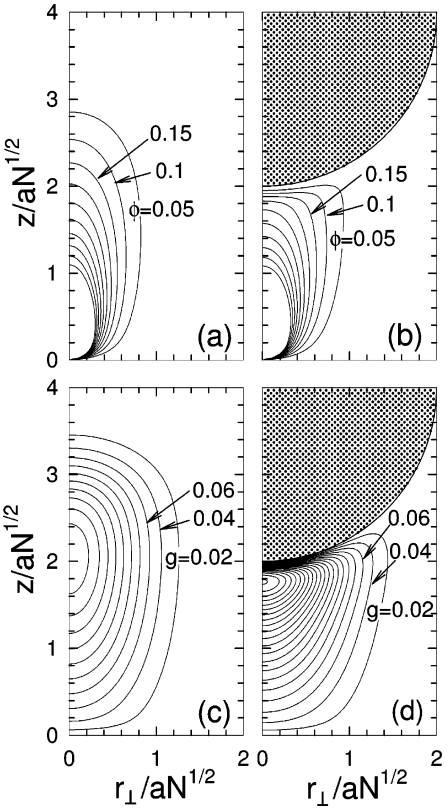

Figure 5. Polymer concentration, $\phi(\mathbf{r}; \mathbf{r}')$, of a single chain grafted at $r'_\perp = 0$ and $z' = \epsilon$ in a brush of thickness $L_0 = 3aN^{1/2}$ (a) without and (b) with a particle of radius $R = 2aN^{1/2}$ at $L = 2aN^{1/2}$. For clarity, the equi-concentration contours are omitted for $\phi > 0.5$. Plots (c) and (d) show the corresponding contour plots for the end-segment distribution, $g(\mathbf{r}; \mathbf{r}')$.

that $l(r_\perp)$ remains nearly constant over lateral distances of $aN^{1/2}$.

The slow convergence does not bode well for the utility of the Derjaguin approximation. However, it is the force that concerns us most, and fortunately the Derjaguin approximation will prove to be far more successful in this regard. Its estimate of the force, eq 32, only requires the free energy penalty of a uniformly compressed brush, which is plotted in Figure 6 for SCFT and SST. As expected, the SCFT predictions approach the SST result (dashed curve) in the limit of $L_0 \to \infty$, but this convergence is again rather slow. For the realistic brush thicknesses considered in Figure 6, the SCFT interaction begins well before $L = L_0$ due to significant fluctuations about the classical trajectories.[17,31] The resulting underestimation by SST never really improves even for relatively high compressions.

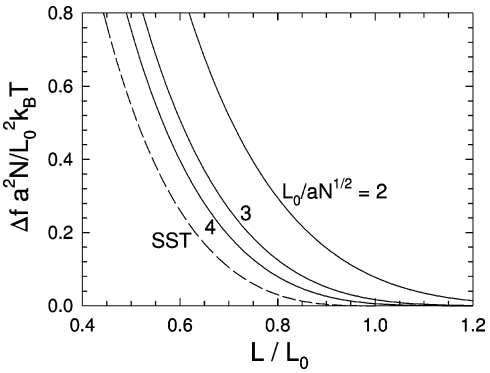

Figure 6. Free energy penalty per chain, Δf, of a brush as a function of uniform compression, L, plotted for several classical brush thicknesses, L_0. The dashed curve denotes the $L_0 \to \infty$ limit given by SST in eq 24.

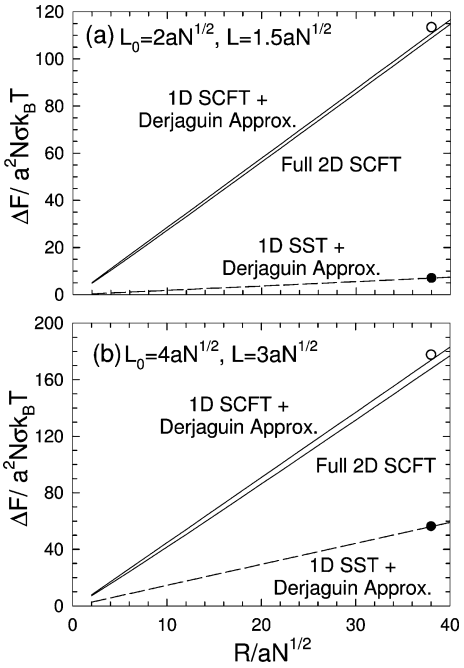

Figure 7. (a) Free energy penalty, ΔF, as a function of particle size, R, for a brush thickness of $L_0 = 2aN^{1/2}$ compressed to a height of $L = 1.5aN^{1/2}$. Curves are shown for the full SCFT calculation as well as the Derjaguin approximation in eq 27 using both SCFT and SST. The symbols compare the further approximation in eq 29. (b) Analogous results for $L_0 = 4aN^{1/2}$ and $L = 3aN^{1/2}$.

The compression by finite-sized particles is examined in Figure 7a, by plotting the free energy penalty vs particle radius at a separation of $L = 1.5aN^{1/2}$ and a typical brush thickness of $L_0 = 2aN^{1/2}$. This plot tests the linear dependence on R predicted by the Derjaguin approximation in eq 29, which gives a straight line passing from the origin through the open circle. This and the more accurate Derjaguin approximation in eq 27 both agree nicely with the SCFT prediction using the full 2-dimensional calculation. Furthermore, the agreement extends down to particle sizes of $R \gtrsim 2aN^{1/2}$, which is remarkably better than the previous performance regarding the segment concentrations. If we, however, use the Derjaguin approximation with SST, eq 27 gives the dashed curve while eq 29 predicts a straight line through the filled circle. Although these SST results are consistent with each other, they are more than an order of magnitude too small. Figure 7b shows analogous results for a brush of twice the thickness, $L_0 = 4aN^{1/2}$, at the same relative compression. As expected, the SST-based predictions become more accurate, but they still underestimate the interaction by a factor of ~3 even

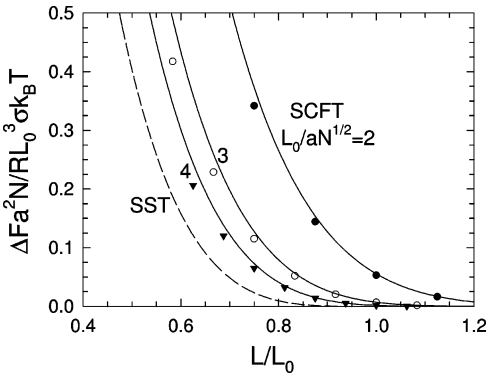

Figure 8. Free energy penalty, ΔF, as a function of compression, L, for particles of radius $R = 10aN^{1/2}$. The filled circles, open circles and filled triangles are calculated with the full SCFT for brushes of thicknesses, $L_0/aN^{1/2} = 2$, 3 and 4, respectively. The solid curves compare the Derjaguin approximation in eq 29 using SCFT, while the dashed curve does the same using SST.

though the brush thickness is beyond typical experimental conditions.

Now that the linear dependence, $\Delta F \propto R$, has been established, Figure 8 examines the energy penalty, ΔF, as a function of compression, L, for particles of a fixed radius, $R = 10aN^{1/2}$. Again the full 2-dimensional SCFT predictions (symbols) are well estimated by the Derjaguin approximation in eq 29 when $\Delta f(l)$ is supplied by SCFT (solid curves); even for this modest particle size, the difference is only a few percent. On the other hand, the SST-based prediction in eq 30 (dashed curve) seriously underestimates the interaction energy for brushes of realistic thickness.

IV. Discussion

Our full 2-dimensional SCFT calculation removes the requirement of large particle radius, R, by the Derjaguin approximation and large brush thickness, L_0, by the SST. Nevertheless, there still remain a few conditions that any application must adhere to. For instance, the spacing between grafting points must be small enough (i.e., $\sigma^{-1/2} \ll aN^{1/2}$) to ensure sufficient overlap among the chains to justify our mean-field treatment, and the brush must be semidilute (i.e., $\lesssim$30% concentration) for the self-consistent field condition in eq 5 to be valid. The polymers should also be flexible (i.e., many persistent lengths long) and not overly extended (i.e., much longer than L_0) for the Gaussian chain model to apply. We have also assumed a neutral particle, but an affinity for the solvent is unlikely to have any significant effect other than to slightly widen the depletion zone. On the other hand, a significant tendency to adsorb polymer will modify the interaction.[5]

Experimental brushes generally have unperturbed heights in the range, $L_0/aN^{1/2} \approx 1-3$.[5−8] Under such conditions, the SST is the dominant source of inaccuracy in the analytical prediction, eq 30, for the repulsive interaction. Of course, this is inevitable given how the SST seriously underestimates the range and strength of $\Delta f(l)$ in Figure 6. Whitmore and Baranowski[18] also found similar problems with SST, although not quite as extreme because they presented their results in a way that masks some of the differences with SCFT. Experimental comparisons[5,6] to SST seem much better partly because they have been done on a logarithmic scale, but sizable discrepancies are still apparent at low compressions. These can supposedly be remedied by accounting for polydispersity,[33] but there are inconsistencies in the parameters used to attain this agreement.[34] In any case, the difference with experiment is a convolution of numerous inaccuracies from both assumptions in the underlying model and uncertainties in N, a, ν, and σ. On the other hand, our comparison with SCFT is done using the identical model with the same exact parameters, and thus the discrepancy with SCFT reveals a purely mathematical inaccuracy caused by restricting the polymers to their classical trajectories.

The scaling theory of Alexander and de Gennes[11] has also had reasonable success in explaining experimental results.[4−7] For uniform compression, it predicts a free energy penalty per chain of

$$\frac{\Delta f(l)}{k_BT} \sim L_0\sigma^{1/2}\left[\frac{7}{12}\left(\frac{l}{L_0}\right)^{-5/4} + \frac{5}{12}\left(\frac{l}{L_0}\right)^{7/4} - 1\right] \qquad (33)$$

to within a prefactor of order unity.[35] Unlike the SCFT and SST calculations, which use the Gaussian chain model, the scaling theory does account for self-avoidance on small length scales (defined by the so-called blob size, $\xi_{blob} \sim \sigma^{-1/2}$), but this one extra consideration cannot justify the crude assumption of a uniform concentration profile.[33] The theory undoubtedly owes its success to the fact that the comparisons are done using L_0 and the amplitude as fitting parameters. If we treat L_0 and σ as fitting parameters, SCFT produces a better fit to the experiments of Klein and co-workers[5−7] than either scaling theory or SST.

Similar comparisons have also been done with simulations. Murat and Grest[13] found that the functional forms of $\Delta f(l)$ predicted by the scaling theory and SST perform equally well, but for SST they set L_0 to the actual brush height rather than the classical height obtained by fitting to a parabolic profile. Toral et al.[36] did not compare their simulations with the scaling theory, but they did find consistent agreement with SST although with an arbitrary prefactor. In a third simulation study by Goujon et al.,[14] scaling theory actually performed somewhat better than SST; once again they only tested the functional form of the theoretical predictions. It should be noted that the small molecular weights used in these simulations do not fully justify comparison to the Gaussian chain model, particularly in the later case[14] where L_0 was not that much greater than the contour length of the polymers.

The generally accepted criterion[37] for the Derjaguin approximation is that the radius of curvature, R, is much larger than the range of the interaction, L_0, and therefore we should not necessarily expect it to be accurate for submicron-sized particles. However, our comparisons with the full 2-dimensional SCFT calculation demonstrate that it can be used on much smaller particles, at least for predicting the force. We have found that reasonable predictions (i.e., ~10% accuracy) can be obtained for radii that are just a couple times larger than $aN^{1/2}$, the typical width over which chains fluctuate in the lateral direction (see Figure 5). For the case of thick brushes, the equator of the particle must also remain well above the brush, such that $\Delta f(l) \approx 0$ before the slope of $l(r_\perp)$ diverges. This results in the more relaxed criteria

$$R \gtrsim 2aN^{1/2} \quad \text{and} \quad R \gtrsim 2(L_0 - L) \qquad (34)$$

Note that when the approximation is pushed to such limits, it is best to use eq 27 rather than eq 29. Of course, our conclusions are specific to the particular geometry in Figure 1, but there is every reason to expect the Derjaguin approximation to perform similarly well in other brush applications.

In the SST, the Derjaguin approximation equates to an assumption that the classical trajectories follow straight vertical paths from the grafting surface. Given the chance, the polymer trajectories would curve away from the particle in order to

reduce the free energy. Thus, the Derjaguin approximation provides an upper bound for ΔF, and so the true 2-dimensional SST prediction would be even smaller than the dashed curves in Figures 7 and 8. This argument does not strictly extend to the SCFT, because of the finite width of the individual polymer profiles, $\phi(\mathbf{r}; \mathbf{r}')$, as shown in Figure 5. Nevertheless, the full SCFT calculation does predict a softer repulsion than the SCFT-based Derjaguin approximation, except for very small particles with $R \lesssim aN^{1/2}$. However, the reduction in ΔF is very slight, despite the considerable lateral displacement of segments that occurs in the full SCFT (compare Figures 2 and 3). This is analogous to what happened in an earlier SST calculation for the interaction between two brush-coated spheres.[29] Evidently, there is a weak sensitivity to the details of the polymer trajectories that allows the Derjaguin approximation to accurately predict the interaction force for much smaller particles than one should realistically expect.

V. Summary

The steric repulsion on a spherical particle by a planar polymer brush has been predicted using the standard Gaussian chain model for high-molecular-weight polymers with a mean-field treatment appropriate to semidilute brushes. It has been common practice to estimate such forces analytically by adapting the strong-stretching theory (SST) of Milner, Witten, and Cates[12] for uniform compression to curved geometries using the Derjaguin approximation.[10] The SST requires the brush thickness, L_0, to be large relative to the characteristic polymer size, $aN^{1/2}$, but small relative to the polymer contour length. The Derjaguin approximation assumes the particle radius, R, is large relative to L_0. Here these assumptions have been removed by using the full numerical self-consistent field theory (SCFT), which reduces to a 2-dimensional computation due to the axial symmetry (see Figure 1).

The full SCFT treatment allowed us to consider particles of small radii and brushes with realistic grafting densities, and it also gave us the opportunity to test the validity of the SST and Derjaguin approximation. For realistic grafting densities, the SST seriously underestimates the free energy penalty for uniform compression, Δf, by typically an order of magnitude. Although the Derjaguin approximation does not predict the perturbation on the composition profile particularly well, it does provide a good estimate of the compression force on nanosized particles when the uniform compression is supplied by a 1-dimensional SCFT calculation. Not only is this approach computationally efficient, it also has the versatility to handle with equal ease particles without axial symmetry, for which the full SCFT would become a costly 3-dimensional computation.

Acknowledgment. This work was supported by the EPSRC (EP/D031494/1).

References and Notes

(1) Milner, S. T. *Science* **1991**, *251*, 905.
(2) Napper, D. H. *Polymeric Stabilisation of Colloidal Dispersions*; Academic Press: London, 1983. Russel, W. B.; Saville, D. A.; Schowalter, W. R. *Colloidal Dispersions*; Cambridge University Press: Cambridge, U.K., 1989.
(3) Sheth, S. R.; Leckband, D. *Proc. Natl. Acad. Sci. U.S.A.* **1997**, *94*, 8399. McPherson, T.; Kidane, A.; Szleifer, I.; Park, K. *Langmuir* **1998**, *14*, 176. Halperin, A. *Langmuir* **1999**, *15*, 2525. Szleifer, I.; Carignano, M. A. *Macromol. Rapid Commun.* **2000**, *21*, 423.
(4) Drobek, T.; Spencer, N. D.; Heuberger, M. *Macromolecules* **2005**, *38*, 5254.
(5) Taunton, H. J.; Toprakcioglu, C.; Fetters, L. J.; Klein, J. *Macromolecules* **1990**, *23*, 571. Taunton, H. J.; Toprakcioglu, C.; Fetters, L. J.; Klein, J. *Nature (London)* **1998**, *332*, 712.
(6) Tadmor, R.; Janik, J.; Klein, J.; Fetters, L. J. *Phys. Rev. Lett.* **2003**, *91*, 115503.
(7) Taunton, H. J.; Toprakcioglu, C.; Klein, J. *Macromolecules* **1988**, *21*, 3336.
(8) Schorr, P. A.; Kwan, T. C. B.; Kilbey, S. M.; Shaqfeh, E. S. G.; Tirrell, M. *Macromolecules* **2003**, *36*, 389.
(9) Nnebe, I. M.; Schneider, J. W. *Macromolecules* **2006**, *39*, 3616.
(10) Derjaguin, B. V. *Kolloid Z.* **1934**, *69*, 155.
(11) Alexander, S. *J. Phys.* (*Fr.*) **1977**, *38*, 983. de Gennes, P. G. *Macromolecules* **1980**, *13*, 1069.
(12) Milner, S. T; Witten, T. A.; Cates, M. E. *Europhys. Lett.* **1988**, *5*, 413. Milner, S. T; Witten, T. A.; Cates, M. E. *Macromolecules* **1988**, *21*, 2610.
(13) Murat, M.; Grest, G. *Phys. Rev. Lett.* **1989**, *63*, 1074.
(14) Goujon, F.; Malfreyt, P.; Tildesley, D. J. *Chem. Phys. Chem.* **2004**, *5*, 457. Goujon, F.; Malfreyt, P.; Tildesley, D. J. *Mol. Phys.* **2005**, *103*, 2675.
(15) Fredrickson, G. H.; Ajdari, A.; Leibler, L.; Carton, J. -P. *Macromolecules* **1992**, *25*, 2882.
(16) Guffond, M. C.; Williams, D. R. M.; Sevick, E. M. *Langmuir* **1997**, *13*, 5691.
(17) Kim, J. U.; Matsen, M. W. *Eur. Phys. J. E* **2007**, *23*, 135.
(18) Whitmore, M. D.; Baranowski, R. *Macromol. Theory Simul.* **2005**, *14*, 75.
(19) Matsen, M. W. In *Soft Matter*; Gompper, G., Schick, M., Eds.; Wiley-VCH: Weinheim, Germany, 2006; Vol. 1; Ch. 2. Fredrickson, G. H. *Equilibrium Theory of Inhomogeneous Polymers* Clarendon Press: Oxford, U.K., 2006.
(20) Edwards, S. F. *Proc. Phys. Soc. London* **1965**, *85*, 613.
(21) Milner, S. T. *J. Chem. Soc. Faraday Trans.* **1990**, *86*, 1349.
(22) Whitmore, M. D.; Noolandi, J. *Macromolecules* **1990**, *23*, 3321.
(23) Roan, J. *Phys. Rev. Lett.* **2001**, *86*, 1027. Roan, J.; Kawakatsu, T. *J. Chem. Phys.* **2002**, *116*, 7283. Roan, J.; Kawakatsu, T. *J. Chem. Phys.* **2002**, *116*, 7295.
(24) Press, W. H.; Teukolsky, S. A.; Vetterling, W. T. *Numerical Recipes in C: the Art of Scientific Computing*; Cambridge University Press: Cambridge, U.K., 1993.
(25) Thompson, R. B.; Rasmussen, K. Ø.; Lookman, T. *J. Chem. Phys.* **2004**, *120*, 31.
(26) Semenov, A. N. *JETP* **1985**, *61*, 733.
(27) Zhulina, E. B.; Boisov, O. V.; Pryamitsyn, V. A.; Birshtein, T. M. *Macromolecules* **1991**, *24*, 140.
(28) Witten, T. A. *Macromol. Rep.* **1992**, *A29*, 87. Solis, F. J.; Tang, H. *Macromolecules* **1996**, *29*, 7953.
(29) Matsen, M. W. *J. Chem. Phys.* **2004**, *121*, 1938.
(30) Kim, J. U.; O'Shaughnessy, B. *Phys. Rev. Lett.* **2002**, *89*, 238301. Kim, J. U.; O'Shaughnessy, B. *Macromolecules* **2006**, *39*, 413.
(31) Milner, S. T.; Witten, T. A. *Macromolecules* **1992**, *25*, 5495.
(32) Joanny, J. F.; Leibler, L.; de Gennes, P. G. *J. Polym. Sci., Polym. Phys.* **1979**, *17*, 1073.
(33) Milner, S. T. *Europhys. Lett.* **1988**, *7*, 695.
(34) The fit in ref 33 uses a brush height of $h_0 = 662$ and free energy per chain of $f_0/\sigma = 12$, but the quoted parameters, $N \equiv N_w/104 = 1356$, $\sigma = 0.00015$, $w = 8.4$, and $\upsilon = 0.052$, predict $h_0 = 419$ and $f_0/\sigma = 5$ (in units of Å and k_BT).
(35) de Gennes, P. G. *Adv. Colloid Interface Sci.* **1987**, *27*, 189.
(36) Toral, R.; Chakrabarti, A.; Dickman, R. *Phys. Rev. E* **1994**, *50*, 343.
(37) McConnell, G. A.; Lin, E. K.; Gast, A. P.; Huang, J. S.; Lin, M. Y.; Smith, S. D. *Faraday Discuss.* **1994**, *98*, 121.

MA071906T